Available online at www.sciencedirect.com

ScienceDirect

journal homepage: http://www.elsevier.com/locate/acme

Original Research Article

Stress intensity factor against fracture toughness in functionally graded geopolymers

A. Nazari *, J.G. Sanjayan

Centre for Sustainable Infrastructure, Faculty of Science, Engineering and Technology, Swinburne University of Technology, Victoria 3122, Australia

ARTICLE INFO

Article history:
Received 24 February 2015
Accepted 28 June 2015
Available online 1 August 2015

Keywords:
Geopolymers
Fracture toughness
Analytical modelling
Stress intensity factor

ABSTRACT

The benefits of producing functionally graded geopolymer in terms of their modified stress intensity factor and fracture toughness are discussed in the present paper. Pre-notched functionally graded geopolymer beams were fabricated by two different fly ash-based geopolymer mixtures. The load was applied parallel to the functionally graded region; two different structures were evaluated by changing the position of the notch. The obtained results indicated that the crack nucleation and growth depend on the interaction between stress intensity factor and fracture toughness. According to the notch position, a crack experience upward or downward variations of properties. When the crack is located in the mixture with the lowest toughness, the variation of properties is called upward and vice versa. A crack facing an upward fracture toughness region is arrested, when the applied stress is equal to the weakest strength of the constituent materials. On the other hand, the fracture toughness of a crack facing a downward fracture toughness gradient is more than that facing an upward one, without any subsequent arresting. It was shown that the position of the notch, and experiencing of downward or upward gradient in mechanical properties mainly determine the final flexural strength of the specimens.

1. Introduction

The concept of functionally graded cementitious materials was first developed in 2006. Especially, first attempts were made to improve flexural fracture of these types of structures. Chen et al. [1] fabricated functionally graded-cellular structures of cement-based materials by co-extrusion which involves extrusion of multiple layers at the same time. They successfully produced three- and five-layer cylindrical cementitious specimens by functionally graded interfaces. Shen et al. [2,3] developed a four-layer polyvinyl alcohol (PVA) fibre-reinforced functionally graded concrete (FGC) by changing the fibre content in the four layers. The specimens then subjected to flexural loading where the maximum content of fibre was used for the surface that is undergone tension. It was concluded that the crack initiation stress increases by using this proposed structure. Roesler et al. [4] also considered fracture

* *Corresponding author*. Tel.: +61 3 92148370.
E-mail address: alinazari@swin.edu.au (A. Nazari).

http://dx.doi.org/10.1016/j.acme.2015.06.005

behaviour of fibre-reinforced FGC specimens and reported improved fracture stress of the pre-notched specimen under flexural three-point loading; however, no considerable compressive and splitting tensile strength was acquired. Park et al. [5] developed a fracture model for functionally graded fibre-reinforced concrete. The finite element simulation was done by differentiating the aggregate bridging zone and the fibre bridging zone. Their results were validated through fabrication of synthetic fibre-reinforced concrete.

Functionally graded concrete specimens by gradual change in the content of fibres were shown to have the desired properties with reduced production costs [6,7]. Apuzzo et al. [8] remark that functionally graded solution can be used to describe the effective constitutive behaviour of composites made of concrete reinforced by steel or polymeric bars. This is evaluated by homogenizing along the plate thickness, and resultant materials are diffusely considered to analyse innovative reinforcing schemes involving modern techniques of seismic rehabilitation. The main benefit of producing FGC specimen with respect to laminated joints is the reduction of stress concentration in the interfaces, where a gradual change of the demanded properties occurs. This is more evident when the FGC specimens are made from different mixtures and constant water to binder ratio. Functionally graded geopolymers (FGG) considered in the present paper are among brittle systems with gradual change in their fracture toughness across the functionally graded region.

Geopolymers are sustainable cement-free construction materials with enhanced mechanical properties and durability and lower embodied energy, greenhouse gases emission and production cost [9–12]. Production of fly ash-based geopolymers, partially or completely from waste materials, breeds waste management as well. Mechanical properties of geopolymers strongly depend on the particle size of the starter ash and Si/Al weight ratio of the alkali-activated mixture [13–15]. FGG specimens in the present study were fabricated by consecutive pouring of two different pastes with different fly ash particle size and Si/Al weight ratios. FGG structures were first introduced in the authors' previous papers [16,17].

Many aspects of functionally graded materials such as free vibration [18], shear deformation [19], thermal buckling [20] and stress intensity factor [21] have been investigated. Fracture toughness of functionally graded sections is of interest especially when a material with elastic behaviour is considered [22,23]. However, the lack of appropriate experimental verifications due to the difficulties in production of the functionally graded sections is the main problem of the literature. Although 3D printing techniques enable producing of functionally graded sections, they are still more appropriate for testing the materials as prototypes. In the present paper, fracture behaviour of FGG specimens with load applied parallel to functionally graded section is considered. Two possible conditions including downward and upward gradient of fracture toughness are investigated. The aim of this study is to develop the concept of FGG more, and to evaluate fracture criteria of these types of structures. Fly ash is used to produce geopolymers because of its availability and much cheaper production cost than other aluminosilicate sources.

2. Geopolymer concrete

Geopolymer is a binder such as ordinary Portland cement (OPC) and the resultant mixture of this binder with appropriate aggregates is called geopolymer concrete. Geopolymers, eco-friendly materials with much lower CO_2 emissions produced from industrial by-products such as fly ash [15], slag [24] or metakaolin [25] are considered as the main possible low carbon alternative to OPC concrete. This has led to significant research in geopolymers in recent years and some field applications, particularly in Australia. Geopolymerisation reaction could create a polymeric backbone of aluminum and silicon atoms where dissolution of aluminosilicate from the basic raw materials occurs [26]. The source of materials used for producing this eco-friendly structure could be completely provided from waste materials such as waste fly ash and waste blastfurnace slags [27]. It is worthwhile to mention that some specific types of fly ash or blastfurnace slags are considered as valuable sources for partial substitution of OPC. Production of geopolymers is carried on ambient temperatures and the produced ceramic-like structure could be used as concrete substitutes, fire-resistant panels as well as media for encapsulation and removal of waste material and hence decreasing the hazards [28]. In the recent years, the demands for geopolymeric specimens have increased. A literature survey from the Scopus databases showed that the scientific publication in the field of geopolymer has been increased five times from 2005 to 2010. It is anticipated that the increase will continue in the ongoing years. The fact may be related to the environmentally friendly nature of these materials, where emission of CO_2 is much lower than that generated during production of concrete specimens from OPC [28–30]. It is amazing that production of 1 ton OPC reveals 1 ton CO_2 directly [31] and where production of OPC reached 3.3 billion tons in 2010 [32,33], this may cause serious problems for the whole globe.

Although the number of buildings made of geopolymer concrete is limited, numerical studies (like this paper) can show their capabilities on developing geopolymeric structures. Geopolymers made for constructional usage are mainly from fly ash. Other materials which are used for production of geopolymers are silica-rich solutions (such as sodium silicate or potassium silicate) and high concentration alkali solutions (such as sodium hydroxide or potassium hydroxide). Combinations of silica rich solution and alkali solution namely alkali activator is mixed by fly ash and makes binders. Geopolymers can gain strength equal to or higher than normal OPC concrete.

To produce geopolymer concrete, many materials such as aluminosilicate source (fly ash, slags, metakaolin, volcanic ash, silica fume and so on), silica-rich solutions (such as sodium of potassium silicate), highly concentrated alkali solutions (such as sodium or potassium hydroxide), different aggregates, fillers, admixtures, superplasticizers and fibres are used. Since the aim of this paper is to investigate the most common used mixtures, only those materials utilized for a normal geopolymer concrete are investigated.

2.1. *Fly ash*

Fly ash is a by-product from combustion of coal which contains fine particles arisen from flue gases. Those particles

that do not come with flue gases are called bottom ash. Depending on the source and makeup of the coal being burned, the components of fly ash vary considerably, but all fly ash includes substantial amounts of SiO_2 (both amorphous and crystalline) and CaO. Fly ash is classified to class F and class C fly ash according to the CaO content [15,24]. While class F fly ash has low contents of CaO, class C fly ash normally contains more than 20 wt.% CaO. Calcium-(sodium)-aluminosilicate-hydrate [C-(N)-A-S-H] and sodium-aluminosilicate-hydrate (N-A-S-H) are the most possible amorphous gels forms during geopolymerization of class C and class F fly ash respectively. Geopolymer concrete made from both types of fly ash may have compressive strength values ranging from medium to high strength. Fly ash is naturally low reactive material and in most cases, fly ash-based geopolymers are produced by oven curing. Oven-cured geopolymers gain their maximum strength at early ages [15,24,26].

2.2. Alkali activator

Alkali activator is a term that is used for a combination of a silica-rich solutions (such as sodium of potassium silicate) and highly concentrated alkali solutions (such as sodium or potassium hydroxide) with certain weight ratios. This combination is used to dissolve fly ash particles and build the amorphous structure of geopolymers. By increasing the ratio of silica-rich solution to alkali solution, the possibility of geopolymerization increases as a result of high amount of SiO_2. For many aluminosilicate sources, it has been proved that availability of SiO_2 is a key factor to determine mechanism of geopolymerization [29]. On the other hand, when high concentrations of alkali solutions are used, dissolution of Si^{4+} and Al^{3+} from fly ash into alkali activator and subsequent formation of geopolymeric structure is higher [34]. However, both of using high amount of silica-rich solution and high concentration of alkali solutions causes unaffordable geopolymer concrete.

2.3. Aggregates

All of aggregates used for OPC concrete can be successfully used for geopolymer concrete. These include but are not limited to river sand, basalt, lightweight aggregates, gravel, crushed stone, slag, recycled aggregates, artificial aggregates and geo-synthesized aggregates. Since near 80 wt.% of a concrete is aggregate, properties of a concrete mainly depends on the aggregates used. However, a suitable geopolymeric binder from a reliable aluminosilicate source can help increasing performance of geopolymer concrete significantly.

3. Experimental procedure to analyse fracture toughness of FGG specimens

3.1. Materials

Specimen production was in accordance to the previous papers [16,17]. FGG specimens were fabricated via consecutive pouring of two different geopolymers mixtures namely G1 and G2. G1 was a mixture of three parts of fly ash type I with average particle size of 14 micron and the Burnauer–Emmett–Teller (BET) specific surface of 85.6 m^2/g and one part of alkali activator. The alkali activator was a mixture of NaOH with concentration of 14 M and sodium silicate containing 37.8% SiO_2 and 12.3% Na_2O. Sodium silicate to NaOH weight ratio was considered 2.5. G2 specimen was produced by the same alkali activator and fly ash type II with average particle size of 9 μm and BET specific surface of 43.8 m^2/g. In Fly ash type I, SiO_2, Al_2O_3, Fe_2O_3, CaO, SO_3, and Na_2O were 35.2, 23.2, 12.3, 20.1, 2.3 and 0.3% respectively, and in Fly ash type II were 62.7, 22.1, 2.5, 3.1, 0.5 and 0.4% respectively. L.O.I for fly ash type I and type II was 3.4 and 2.6% respectively.

3.2. Mixture preparation

G1 and G2 monolithic specimens were made by pouring the mixture into the moulds in two layers and subsequent 45 s vibration. Two types of FGG specimens were fabricated with 20 and 80 volume fraction of G1 mixture. At first, G1 mixture was introduced to the mould and vibrated for 45 s. Afterward, G2 mixture was poured as the top layer and vibrated for additional 45 s. Functionally graded strip forms during vibration and subsequent hardening process. All the mixtures were pre-cured for 24 h in the moulds covered by a polyester sheet and then, were oven-cured for 6 h at 90 °C. Finally, they were cured at room temperature for additional 28 days.

3.3. Mechanical tests

Fracture toughness of the samples was achieved by a single-notched edge beam under three-point loading with the dimensions of 10 cm × 10 cm × 65 cm. The span to depth ratio was 4 and width and tip radius of the crack were 5 and 1 mm respectively. At first, the thickness of the specimens was considered more than 10 cm. After determining the depth of functionally graded region, the specimens were cut in such a way those only contain a monolithic region and a functionally graded region. In other words, in the structure called FGG1, the specimen contained only G1 monolithic layer and functionally graded region. In the other structure called FGG2, the specimen consisted of G2 monolithic layer and functionally graded region. These proposed structures are shown schematically in Fig. 1. Additionally, the load in the FGG specimens applied parallel to the functionally graded region. The term fracture toughness is the required energy for crack initiation and growth. According to the standard test procedures, fracture toughness is measured by a pre-notched specimen. In this paper, ASTM E1820 was followed to determine fracture toughness of FGG and monolithic specimens. Fracture toughness of specific materials depends on the applied load, initial crack length and specimen's dimensions. For the structure of Fig. 1, the fracture toughness, K_C, of the monolithic specimens is calculated in accordance to Eq. (1) [35]:

$$K_C = \frac{4P_{max}}{B}\cdot\sqrt{\frac{\pi}{W}}\left[1.6\left(\frac{a_0}{W}\right)^{1/2} - 2.6\left(\frac{a_0}{W}\right)^{3/2} + 12.3\left(\frac{a_0}{W}\right)^{5/2} - 21.2\left(\frac{a_0}{W}\right)^{7/2} + 21.8\left(\frac{a_0}{W}\right)^{9/2}\right] \quad (1)$$

where P_{max} is the maximum applied load, B is the thickness of the specimen, W is the specimen width, and a_0 is the initial crack length.

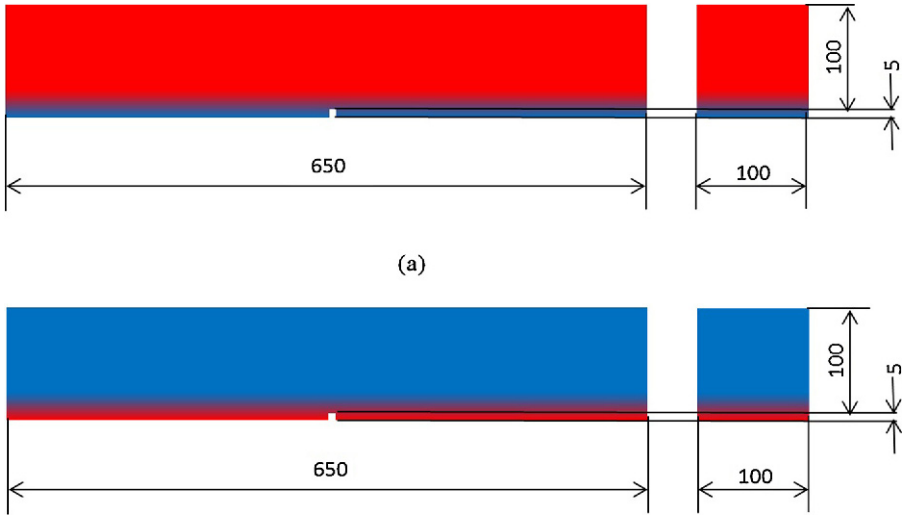

Fig. 1 – Schematic illustration of (a) FGG1 and (b) FGG2 specimens (Dimensions in mm). Blue: G1 monolithic layer, Red: G2 monolithic layer. Gradient fill: Functionally graded region.

Fracture toughness tests were conducted by an Instron universal machine. Five samples were tested for each mixture and the average maximum load was reported for the specimens.

3.4. *Determining the size of functionally graded region*

The depth of functionally graded layer was determined by an innovative method using scanning electron microscopy (SEM) equipped with energy dispersive spectroscopy (EDS) facility. Monolithic G1 and G2 specimens were analysed by EDS and their average Si/Al peak ratio were obtained through 10 analyses. To determine the functionally graded depth, several imaginary parallel lines were drawn on the specimen's SEM pattern by interval of 50 μm, and Si/Al ratio of the 10 selected points on each line were achieved. The average Si/Al ratio of these 10 points was considered as the average Si/Al ratio of that line. The boundaries of the functionally graded region were considered those lines with 5% Si/Al alteration with respect to G1 and G2 monolithic specimens. The depth (the term depth is used because gradual change of properties occurs in specimen's depth) of functionally graded region was equal to 1.86 cm and more comprehensive description can be achieved through Refs. [16,17].

4. Results and discussion

P_{max} of G1, G2, FGG1 and FGG2 specimens were 8.79, 13.6, 9.80 and 13.2 kN, respectively. Thickness of specimen, specimen width and crack length were 100, 100 and 5 mm respectively for all G1, G2, FGG1 and FGG2 specimens. Accordingly, fracture toughness calculated by Eq. (1) for G1 and G2 specimens was 0.66 and 1.02 MPa $\sqrt{m}$ respectively. Furthermore, Young's modulus of G1 and G2 specimens was 33 and 42 GPa respectively obtained in the authors' previous paper according to the ASTM C469-87 standard [16]. The results show that P_{max} of both FGG specimens is an amount between that of G1 and G2 monolithic specimens. Although fracture toughness of monolithic specimens is calculated, according to the following discussion, Eq. (1) cannot be simply used to determine the fracture toughness of the FGG specimens. In other words, $P_{max}\sigma_f$ obtained from the experiments cannot be simply substituted into Eq. (1) and more detailed solutions are required. As a guide, fracture toughness of FGG1 and FGG2 specimens were calculated by Eq. (1) and they were equal to 0.74 and 0.99 MPa $\sqrt{m}$ respectively. However, as the following discussion will show, fracture toughness in functionally graded regions is a function rather than a single value.

Variations of mechanical properties in the functionally graded region may be presented by different functions especially in elastic sections, where determining the mechanical properties is difficult. Three types of functions are normally utilized for representing the variations of fracture toughness in functionally graded region including exponential (Eq. (2)), linear (Eq. (3)) and logarithmic (Eq. (4)), where their type of variation is schematically illustrated in Fig. 2. All of these equations show the nature of a functionally graded material. These equations show that specific properties (here fracture toughness) change gradually across the thickness of functionally graded region. Where the variations of properties in functionally graded sections are not easily detectable, some popular functions are used. Most of the solutions in the literature show that using a pre-defined function does not cause a significant deviation in modelling procedure.

$$K_{C,FGG} = A\exp(Bt) \tag{2}$$

$$K_{C,FGG} = At + B \tag{3}$$

$$K_{C,FGG} = A\ln(Bt) \tag{4}$$

where $K_{C,FGG}$ is the fracture toughness in functionally graded region and t is the distance from the notch tip. A and B are constants determined by considering suitable boundary

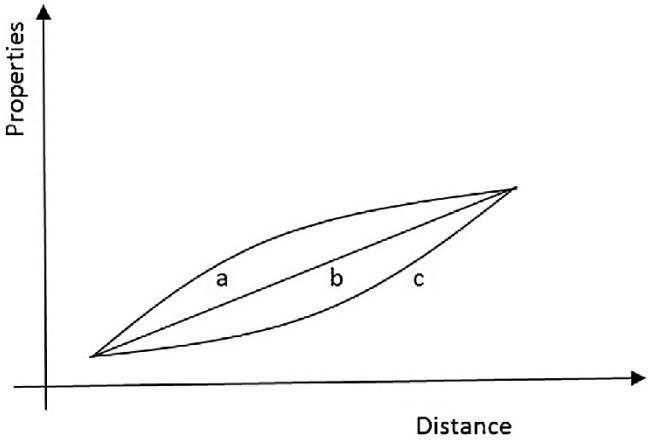

Fig. 2 – Schematic illustration of the properties variations in functionally graded region. (a) logarithmic variations, (b) linear variations and (c) exponential variations.

conditions. For a functionally graded section, the following boundary conditions may apply:

If $t = t_{G1} =$ then $K_{C,FGG} = K_C^{G1}$,

and

If $t = t_{G1} =$ then $K_{C,FGG} = K_C^{G1}$,

where K_C^{G1} and K_C^{G2} are fracture toughness of G1 and G2 layers and t_{G1} and t_{G2} are the positions of G1 and G2 layers. G1 and G2 layers in the functionally graded section are those layers with the same chemical composition and mechanical properties as G1 and G2 monolithic specimens respectively.

Eqs. (2)–(4) are rearranged as:

$$K_{C,FGG} = K_C^{G1} \cdot \left(\frac{K_C^{G1}}{K_C^{G2}}\right)^{((t-t_{G1})/(t_{G1}-t_{G2}))} \tag{5}$$

$$K_{C,FGG} = \frac{K_C^{G1}(t - t_{G2}) - K_C^{G2}(t - t_{G1})}{t_{G1} - t_{G2}} \tag{6}$$

$$K_{C,FGG} = \frac{K_C^{G1} \cdot \ln(t_{G1}) - K_C^{G2} \cdot \ln(t_{G2}) + (K_C^{G2} - K_C^{G1})\ln(t)}{\ln(t_{G2}/t_{G1})} \tag{7}$$

All of these three functions are suitable for representing the variations of properties in functionally graded region. The authors' previous paper [16] shows that exponential function is more suitable for geopolymers. Therefore, exponential function is selected in this paper to evaluate the variation of all properties in functionally graded region.

Fig. 3 shows schematically the variations of stress intensity factor, K, *vs.* fracture toughness in monolithic specimen and functionally graded region. Fig. 3a shows that the crack initiates when K reaches to its critical value K_C. Same reason is valid for the fracture of functionally graded sections, where the variation of fracture toughness depends on the specimen depth as illustrated in Fig. 3b. Two possible cracks in the FGG specimens with load parallel to the graded region are considered including downward (Fig. 3c) and upward (Fig. 3d) variations of fracture toughness.

Fig. 3c shows that for upward variations of fracture toughness, the stress intensity factor for crack initiation must be higher than its fracture toughness. Therefore, the applied load might be higher than that of required for initiating of crack in monolithic G1 specimen. However, the applied load could be considered less than that required for initiating the crack in monolithic G2 specimen. The interesting point of the proposed applied load model is arresting the crack in a depth where K_C exceeds K. This has been indicated as crack arresting point in Fig. 3c. Therefore, one may fabricate a functionally graded geopolymers from various low and high fracture toughness cured mixtures, where low fracture toughness is required. In this case, when a minimum value of fracture toughness is required, one may ensure that the section carries load up to or even higher its fracture toughness. This is even more beneficial, when the difference between fracture toughness of the tow constituent mixtures is high. Additionally, the section can be produced by cheap and low grade fly ash and reinforced by higher quality more expensive fly ash. The result would be a functionally graded section with lower cost and extremely reduced stress concentration.

Fig. 3d shows that in a functionally graded region with downward fracture toughness variations, the stress intensity factor must be equal or higher than that of required for crack initiation in monolithic G1 specimen. However, after initiating the crack, no arresting point occurs. In other words, the crack initiation requires intensity factor as high as that required for G2 specimen with no subsequent crack arresting. This is an interesting feature, where high fracture toughness is achieved by only using a thin section of high quality G2 specimen. One may use the section with high fracture toughness. However, because of abrupt fracture occurrence due to high stress intensity factor, a safety factor might be identified for these types of applied loads.

Fig. 4 shows the stress intensity factor and fracture toughness variations in the graded region of FGG1 specimen. K_C of the monolithic region is calculated by Eq. (1) and $K_{C,FGG}$ in the functionally graded region is calculated by Eq. (5). The stress intensity factor of the specimen was calculated by the following equation [35]:

$$K = \frac{4P}{B} \cdot \sqrt{\frac{\pi}{W}} \left[1.6\left(\frac{a_i}{W}\right)^{1/2} - 2.6\left(\frac{a_i}{W}\right)^{3/2} + 12.3\left(\frac{a_i}{W}\right)^{5/2} - 21.2\left(\frac{a_i}{W}\right)^{7/2} + 21.8\left(\frac{a_i}{W}\right)^{9/2}\right] \tag{8}$$

where P is the applied load and a_i is the effective crack length at each step.

To calculate K, the specimen was considered as a section containing n parallel layers with the intervals of 50 μm. The effective crack length of each layer was considered as $a_i = a_{i-1} + 0.0005$ (m).

The applied load in Eq. (8) is considered 8.79 kN equal to the maximum load applicable on G1 specimen. According to the fracture mechanic rules, fracture occurs when K reaches to K_C. This is sufficient for crack initiating. However, after initiating the crack, no interaction between K and K_C curves occurs. This means that maximum load of FGG1 specimen should be equal to 8.79 kN and no additional load is required. However, the obtained experimental maximum load of 9.80 kN for FGG1 specimen indicates that a modification is required for the variation of K. K is related to the Young's modulus, E, and

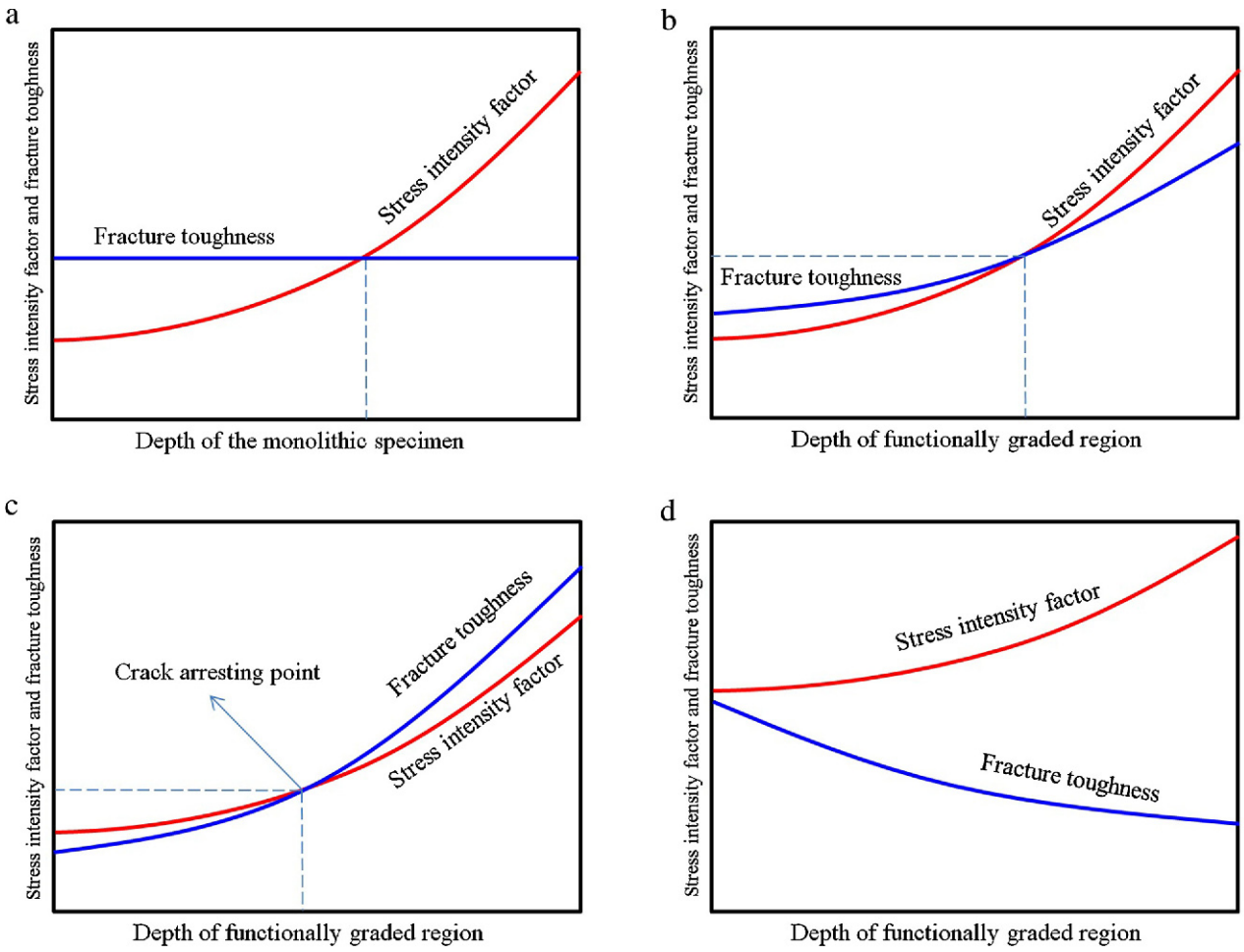

Fig. 3 – Schematic illustration of fracture criteria in (a) monolithic material and (b) functionally graded material. Stress intensity factor *vs.* fracture toughness in specimens with (c) upward fracture toughness variations and (d) downward fracture toughness variation. The term depth means the direction where a specific property changes. This change may occur in length, width or thickness of a specimen.

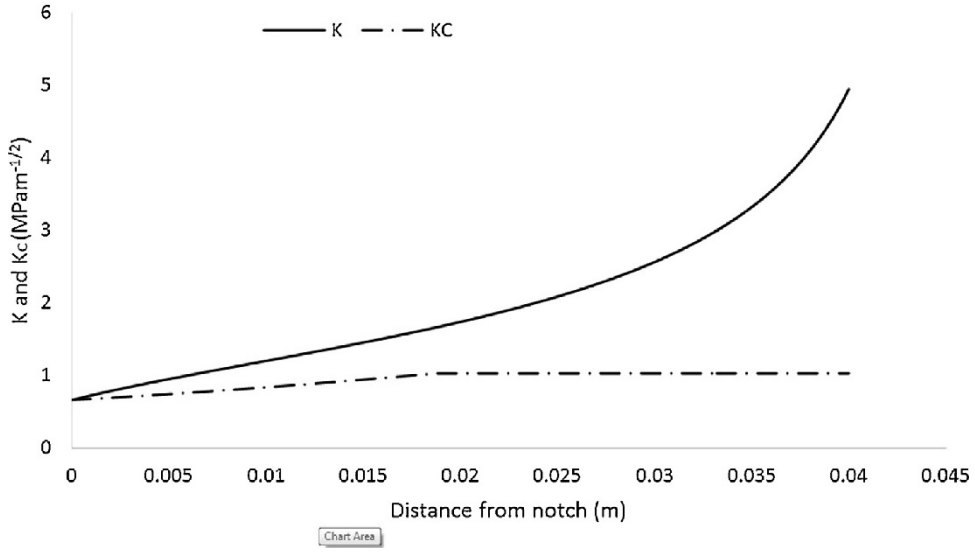

Fig. 4 – Stress intensity factor *vs.* fracture toughness of FGG1 specimen. Distance from notch means the distance between the new and original position of the crack tip.

elastic energy release rate, G, according to Eq. (9), where the Poison's ratio is equal to zero:

$$K = \sqrt{E \cdot G} \tag{9}$$

For the specimens with higher E, at a constant K, G decreases. In other words, stiffer specimens have higher resistance to energy release and hence, higher strength. In other words, while in Eq. (8) the stress intensity factor is considered independent of materials properties, Eq. (9) indicates that these properties must be considered. For stiffer materials with higher E, stress intensity factor is lower. Therefore, a modification factor for functionally graded sections is suggested by authors for Eq. (8) as following:

$$K_{FGG} = A\frac{4P}{B}\cdot\sqrt{\frac{\pi}{W}}\left[1.6\left(\frac{a_i}{W}\right)^{1/2} - 2.6\left(\frac{a_i}{W}\right)^{3/2} + 12.3\left(\frac{a_i}{W}\right)^{5/2} - 21.2\left(\frac{a_i}{W}\right)^{7/2} + 21.8\left(\frac{a_i}{W}\right)^{9/2}\right] \tag{10}$$

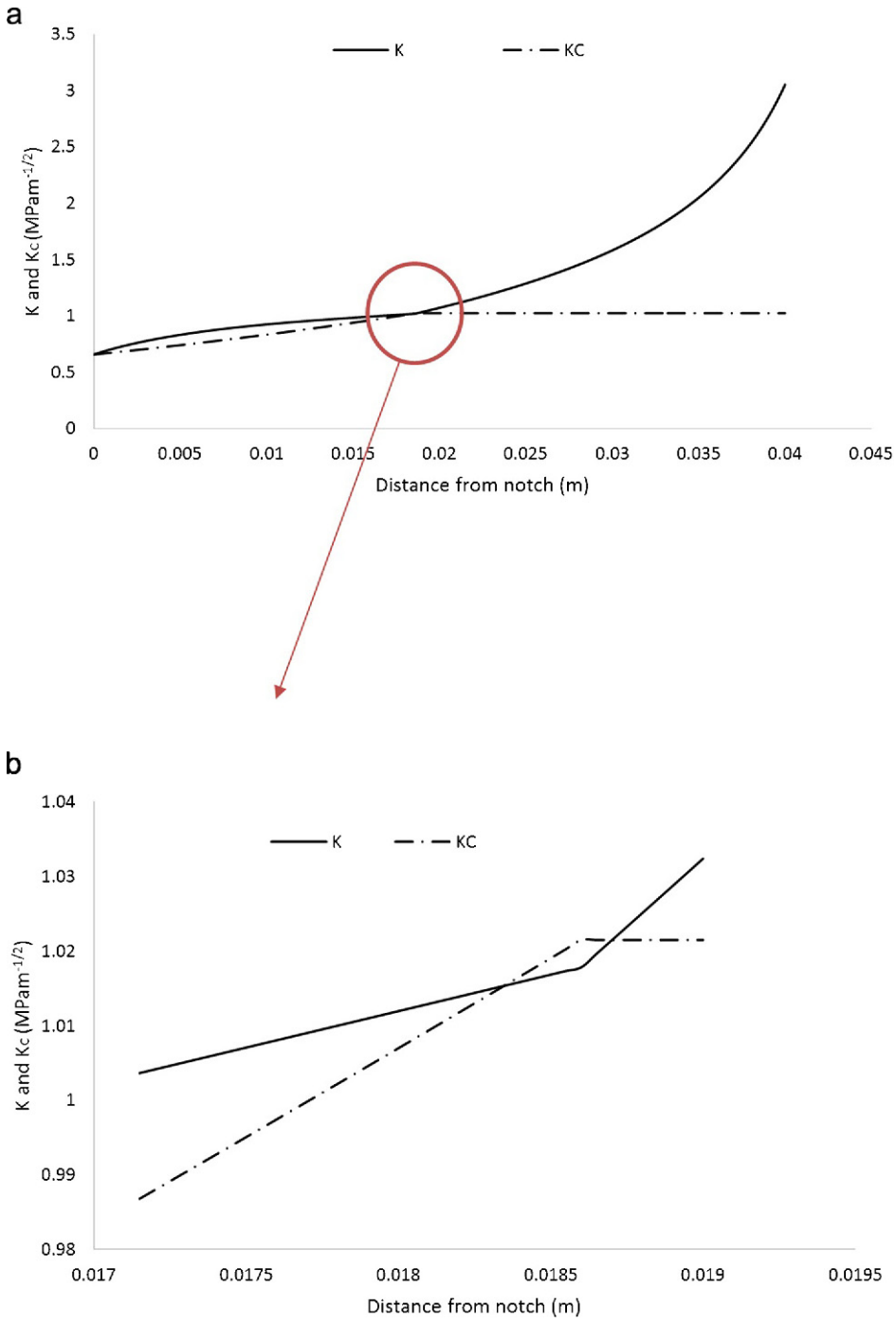

Fig. 5 – (a) Modified stress intensity factor *vs.* fracture toughness of FGG1 specimen, (b) The distance at with *K* is lower than K_C in higher magnification (the part of circle zone of section a). Distance from notch means the distance between the new and original position of the crack tip.

where K_{FGG} is the stress intensity factor of functionally graded region and A is the modification factor.

The simplest modification factor suggested here obtained by trial and error is $Á/E_{FGG}^2$ where Á is a constant and E_{FGG} is the Young's modulus of functionally graded region. By considering that for the weakest E (here, G1 specimen), K in Eqs. (8) and (10) must be equal, the suggested function for functionally graded region is simplified as:

$$K_{FGG} = \frac{4P}{B}\cdot\sqrt{\frac{\pi}{W}}\left[1.6\left(\frac{a_i}{W}\right)^{1/2} - 2.6\left(\frac{a_i}{W}\right)^{3/2} + 12.3\left(\frac{a_i}{W}\right)^{5/2} - 21.2\left(\frac{a_i}{W}\right)^{7/2} + 21.8\left(\frac{a_i}{W}\right)^{9/2}\right]\cdot\frac{E_{G1}^2}{E_{FGG}^2} \quad (11)$$

where E_{G1} is the Young's modulus of G1 monolithic specimen. Eq. (11) shows that fracture toughness of FGG specimen is same as fracture toughness of monolithic sections modified by a ratio of elastic modulus. This indicates the importance of modulus of elasticity in brittle systems, where fracture is controlled by yield strength criteria.

Same as fracture toughness, variations of E_{FGG} in functionally graded region can be presented by exponential (Eq. (12)), function as following. Same as Eqs. (2)–(4), the following equation shows that gradual variation of properties (here, elastic modulus) in functionally graded sections can be identified by a pre-defined function with minimum impact on the accuracy of model.

$$E_{FGG} = C\exp(Dt) \quad (12)$$

where C and D are constants, which are determined by considering suitable boundary conditions. For a functionally graded section, the following boundary conditions may apply:

If $t = t_{G1}$ = then $E_{FGG} = E_{G1}$,

and

If $t = t_{G2}$ = then $E_{FGG} = E_{G2}$

where E_{G2} is the Young's modulus of G2 monolithic specimen. Therefore, Eq. (12) can be rearranged as:

$$E_{FGG} = E_{G1}\cdot\left(\frac{E_{G1}}{E_{G2}}\right)^{((t-t_{G1})/(t_{G1}-t_{G2}))} \quad (13)$$

By utilizing exponential variations of E_{FGG}, Eq. (11) is re-written as:

$$E_{FGG} == \frac{4P}{B}\cdot\sqrt{\frac{\pi}{W}}\left[1.6\left(\frac{a_i}{W}\right)^{1/2} - 2.6\left(\frac{a_i}{W}\right)^{3/2} + 12.3\left(\frac{a_i}{W}\right)^{5/2} - 21.2\left(\frac{a_i}{W}\right)^{7/2} + 21.8\left(\frac{a_i}{W}\right)^{9/2}\right]\cdot\left(\frac{E_{G1}^2}{E_{G2}^2}\right)^{2((t-t_{G1})/(t_{G1}-t_{G2}))} \quad (14)$$

The effect of these variations on functionally graded region will be continued in monolithic G2 section and a decrease in its normal stress intensity factor obtained by Eq. (8) occurs. At the end of functionally graded region, E_{FGG} reaches to E_{G2} and hence, the suggested modification factor becomes E_{G1}^2/E_{G2}^2. Therefore, it is suggested that this factor influences K of the remained monolithic section as following:

$$K_{G2} = \frac{4P}{B}\cdot\sqrt{\frac{\pi}{W}}\left[1.6\left(\frac{a_i}{W}\right)^{1/2} - 2.6\left(\frac{a_i}{W}\right)^{3/2} + 12.3\left(\frac{a_i}{W}\right)^{5/2} - 21.2\left(\frac{a_i}{W}\right)^{7/2} + 21.8\left(\frac{a_i}{W}\right)^{9/2}\right]\cdot\left(\frac{E_{G1}^2}{E_{G2}^2}\right) \quad (15)$$

where K_{G2} is the modified stress intensity factor for G2 monolithic region.

Fig. 5 shows the modified stress intensity factor for FGG1 specimen *vs.* its fracture toughness. There is an interaction between two curves indicating that by a load equal to 8.79 kN, crack is arrested, where K_C exceeds K. Therefore higher stresses are required for crack propagation across the FGG1 specimen justifying the experimental result and subsequent modification.

Fig. 6 shows the stress intensity factor, modified stress intensity factor and fracture toughness of FGG2 specimen. Both K and K_{FGG} have no interaction by K_C because the initial applied stress is considered 13.6 kN equal to the maximum load applicable on G2 monolithic specimen. This indicates that although the specimen mainly contains G1 mixture, initiating of crack requires more stress in G2 layer. This is in accordance

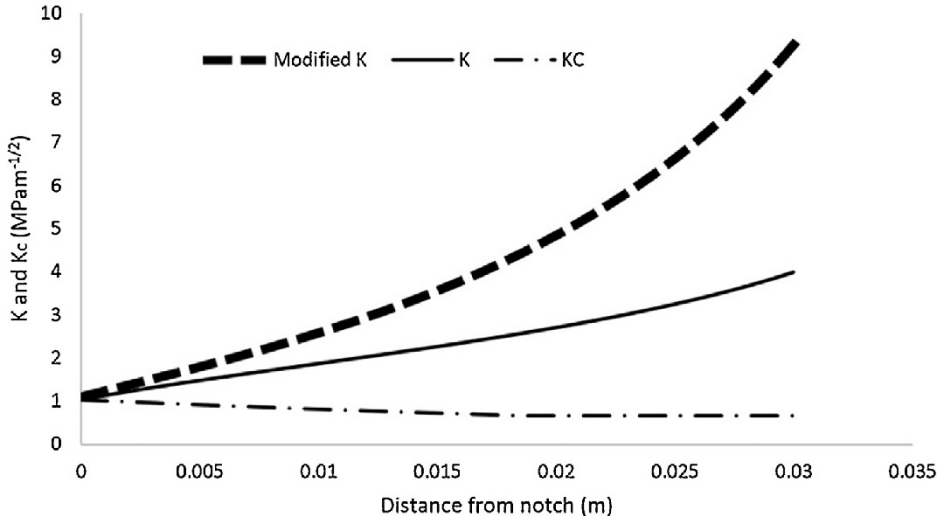

Fig. 6 – Stress intensity factor and modified stress intensity factor *vs.* fracture toughness of FGG2 specimen. Distance from notch means the distance between the new and original position of the crack tip.

to the experimental results, where a maximum load of 13.2 kN was achieved very close to the maximum load applicable on G2 specimen (13.6 kN). The deviation may be related to the experimental errors.

The whole results indicate that making functionally graded geopolymeric specimens has several features inaccessible by a monolithic specimen. It was obtained that the fracture toughness of the specimens depends on the notch tip position rather than the amount of constituent mixture. In other words, to attain high flexural strength, it is possible to use low grade cost-effective fly ash and make a functionally graded surface with high quality fly ash. On the other hand, in FGG specimens with upward changes of properties, it is possible to arrest the crack by applying a high quality geopolymer on a low grade one, where the crack is located in the geopolymeric region made of low grade geopolymer.

5. Conclusions

In the present paper, a modification method was proposed to the variations of stress intensity factor, K, in FGG specimen. At first, fracture toughness, K_C, of functionally graded region was suggested to change exponentially. By intersecting the curves of K and K_C, fracture toughness of functionally graded specimens was determined. However, to deliver a comprehensive formulation of K, a modification procedure was carried on. In addition to the variations of K in functionally graded region, the post monolithic region in FGG is affected by the variation of K in functionally graded region. A modification factor of elastic modulus ratio was proposed to determine the effect of notch position on fracture toughness of specimens. While both specimens consist of G1 and G2 monolithic specimens, the fracture energy strongly depends on the notch tip position. Regardless of the content of constituent materials, upward and downward changes of mechanical properties determine the crack initiating and propagating across the FGG specimens. This modification factor is not observed in most theoretical models and only variation of properties in graded region is considered. However, experimental observations in this paper show this important difference feature.

REFERENCES

[1] Y. Chen, L.J. Struble, G.H. Paulino, Fabrication of functionally graded-cellular structures of cement-based materials by co-extrusion, in: AIP Conference Proceedings, vol. 973, 2008, February, 532.

[2] B. Shen, M. Hubler, G.H. Paulino, L.J. Struble, Manufacturing and mechanical testing of a new functionally graded fiber reinforced cement composite, in: AIP Conference Proceedings, vol. 973, 2008, February, 519.

[3] B. Shen, M. Hubler, G.H. Paulino, L.J. Struble, Functionally-graded fiber-reinforced cement composite: processing, microstructure, and properties, Cement and Concrete Composites 30 (8) (2008) 663–673.

[4] J. Roesler, A. Bordelon, C. Gaedicke, K. Park, G. Paulino, Fracture behavior and properties of functionally graded fiber-reinforced concrete, in: AIP Conference Proceedings, vol. 973, 2008, February, 513.

[5] K. Park, G.H. Paulino, J. Roesler, Cohesive fracture model for functionally graded fiber reinforced concrete, Cement and Concrete Research 40 (6) (2010) 956–965.

[6] X.D. Wen, J.L. Tu, W.Z. Gan, Durability protection of the functionally graded structure concrete in the splash zone, Construction and Building Materials 41 (2013) 246–251.

[7] C.M.R. Dias, H. Savastano Jr., V.M. John, Exploring the potential of functionally graded materials concept for the development of fiber cement, Construction and Building Materials 24 (2) (2010) 140–146.

[8] A. Apuzzo, R. Barretta, R. Luciano, Some analytical solutions of functionally graded Kirchhoff plates, Composites Part B: Engineering 68 (2015) 266–269.

[9] N.W. Chen-Tan, A. Van Riessen, C.V. Ly, D.C. Southam, Determining the reactivity of a fly ash for production of geopolymer, Journal of the American Ceramic Society 92 (4) (2009) 881–887.

[10] I. Ismail, S.A. Bernal, J.L. Provis, S. Hamdan, J.S. van Deventer, Microstructural changes in alkali activated fly ash/slag geopolymers with sulfate exposure, Materials and Structures 46 (3) (2013) 361–373.

[11] A. Kumar, S. Kumar, Development of paving blocks from synergistic use of red mud and fly ash using geopolymerization, Construction and Building Materials 38 (2013) 865–871.

[12] K. Somna, C. Jaturapitakkul, P. Kajitvichyanukul, P. Chindaprasirt, NaOH-activated ground fly ash geopolymer cured at ambient temperature, Fuel 90 (6) (2011) 2118–2124.

[13] Z.X. Yang, J.M. Zhao, K.H. Hwang, S.J. Shin, H.R. Lee, Strength enhancement of sludge based geopolymer by Si/Al ratio variation, Advanced Materials Research 610 (2013) 518–521.

[14] Y.C. Wang, Y.J. Zhang, D.L. Xu, L.C. Liu, Influence of different curing temperatures on mechanical properties of alkali activated silica fume and fly ash based geopolymer, Materials Research Innovations 17 (s1) (2013) s21–s25.

[15] G.S. Ryu, Y.B. Lee, K.T. Koh, Y.S. Chung, The mechanical properties of fly ash-based geopolymer concrete with alkaline activators, Construction and Building Materials 47 (2013) 409–418.

[16] A. Nazari, J.G. Sanjayan, Modelling of fracture strength of functionally graded geopolymer, Construction and Building Materials 58 (2014) 38–45.

[17] A. Nazari, J.G. Sanjayan, Compressive strength of functionally graded geopolymers: role of position of layers, Construction and Building Materials 75 (2015) 31–34.

[18] Y. Liu, D.W. Shu, Free vibration analysis of exponential functionally graded beams with a single delamination, Composites Part B: Engineering 59 (2014) 166–172.

[19] Z. Belabed, M.S. Ahmed Houari, A. Tounsi, S.R. Mahmoud, O. Anwar Bég, An efficient and simple higher order shear and normal deformation theory for functionally graded material (FGM) plates, Composites Part B: Engineering 60 (2014) 274–283.

[20] K.S. Na, J.H. Kim, Three-dimensional thermal buckling analysis of functionally graded materials, Composites Part B: Engineering 35 (5) (2004) 429–437.

[21] W. Zhao, Z. Hu, X. Zhang, H. Xie, L. Yu, The dynamic stress intensity factor around the anti-plane crack in an infinite strip functionally graded material under impact loading, Theoretical and Applied Fracture Mechanics 74 (2014) 1–6.

[22] U.H. Bankar, V. Parameswaran, Fracture of edge cracked layered plates subjected to in-plane bending, Experimental Mechanics 53 (2) (2013) 287–298.

[23] I.V. Ivanov, T. Sadowski, D. Pietras, Crack propagation in functionally graded strip under thermal shock, European Physical Journal Special Topics 222 (7) (2013) 1587–1595.

[24] A. Bagheri, A. Nazari, Compressive strength of high strength class C fly ash-based geopolymers with reactive granulated blast furnace slag aggregates designed by Taguchi method, Materials & Design 54 (2014) 483–490.

[25] A. Autef, E. Joussein, A. Poulesquen, G. Gasgnier, S. Pronier, I. Sobrados, J. Sanz, S. Rossignol, Influence of metakaolin purities on potassium geopolymer formulation: the existence of several networks, Journal of Colloid and Interface Science 408 (2013) 43–58.
[26] W.D. Rickard, R. Williams, J. Temuujin, A. van Riessen, Assessing the suitability of three Australian fly ashes as an aluminosilicate source for geopolymers in high temperature applications, Materials Science and Engineering: A 528 (9) (2011) 3390–3397.
[27] M. Ben Haha, G. Le Saout, F. Winnefeld, B. Lothenbach, Influence of activator type on hydration kinetics, hydrate assemblage and microstructural development of alkali activated blast-furnace slags, Cement and Concrete Research 41 (3) (2011) 301–310.
[28] A.T. Durant, K.J. MacKenzie, Synthesis of sodium and potassium aluminogermanate inorganic polymers, Materials Letters 65 (13) (2011) 2086–2088.
[29] A. Hajimohammadi, J.L. Provis, J.S. van Deventer, The effect of silica availability on the mechanism of geopolymerization, Cement and Concrete Research 41 (3) (2011) 210–216.
[30] M. Romagnoli, C. Leonelli, E. Kamse, M. Lassinantti Gualtieri, Rheology of geopolymer by DOE approach, Construction and Building Materials 36 (2012) 251–258.
[31] J. Davidovits, Geopolymer cements to minimize carbon-dioxide greenhouse warming, in: M. Moukwa, S.L. Sarkar, K. Luke, et al. (Eds.), Ceramic Transactions Cement-Based Materials: Present, Future, and Environmental Aspects, The American Ceramic Society, Westerville, 1993 165–181.
[32] A. Kusbiantoro, M.F. Nuruddin, N. Shafiq, S.A. Qazi, The effect of microwave incinerated rice husk ash on the compressive and bond strength of fly ash based geopolymer concrete, Construction and Building Materials 36 (2012) 695–703.
[33] H.G.V. Oss, Cement. United States Geological Survey: Mineral Commodity Summaries, 2011.
[34] S. Hanjitsuwan, S. Hunpratub, P. Thongbai, S. Maensiri, V. Sata, P. Chindaprasirt, Effects of NaOH concentrations on physical and electrical properties of high calcium fly ash geopolymer paste, Cement and Concrete Composites 45 (2014) 9–14.
[35] A.F. Bower, Applied Mechanics of Solids, CRC Press, Boca Raton, FL, 2009.